J|A|C|S ARTICLES

Published on Web 06/01/2009

Zeolite-Supported Organorhodium Fragments: Essentially Molecular Surface Chemistry Elucidated with Spectroscopy and Theory

Ann J. Liang,[†] Raluca Craciun,[‡] Mingyang Chen,[‡] T. Glenn Kelly,[‡] Philip W. Kletnieks,[§] James F. Haw,*[,§] David A. Dixon,*[,‡] and Bruce C. Gates*[,†]

Department of Chemical Engineering and Materials Science, University of California, Davis, California 95616, Department of Chemistry, University of Alabama, Tuscaloosa, Alabama 35487, and Department of Chemistry, University of Southern California, Los Angeles, California 90089

Received January 4, 2009; E-mail: bcgates@ucdavis.edu; jhaw@usc.edu; dadixon@as.ua.edu

Abstract: Structures of zeolite-anchored organorhodium complexes undergoing conversions with gas-phase reactants were characterized by infrared spectra bolstered by calculations with density functional theory and analysis of the gas-phase products. Structurally well-defined zeolite-supported rhodium diethylene complexes were synthesized by chemisorption of $Rh(C_2H_4)_2(acac)$ (acac = $CH_3COCHCOCH_3$) on dealuminated Y zeolite, being anchored by two Rh−O bonds, as shown by extended X-ray absorption fine structure (EXAFS) spectroscopy. In contrast to the nonuniformity of metal complexes anchored to metal oxides, the near uniformity of the zeolite-supported species allowed precise determination of their chemistry, including the role of the support as a ligand. The anchored rhodium diethylene complex underwent facile, reversible ligand exchange with deuterated ethylene at 298 K, and ethylene ligands were hydrogenated by reverse spillover of hydrogen from support hydroxyl groups. The supported complexes reacted with CO to form rhodium *gem*-dicarbonyls, which, in the presence of ethylene, gave rhodium monocarbonyls. The facile removal of ethylene ligands from the complex in H_2-N_2 mixtures created coordinatively unsaturated rhodium complexes; the coordinative unsaturation was stabilized by the site isolation of the complexes, allowing reaction with N_2 to form rhodium complexes with one and with two N_2 ligands. The results also provide evidence of a new rhodium monohydride species incorporating a C_2H_4 ligand.

Introduction

Oxide-supported metal complexes are a widely investigated and industrially important class of catalyst.[1] Understanding their chemistry is hindered by the complexity of their structures, which is linked to the intrinsic nonuniformity of the support surfaces. To simplify matters, Miessner et al. used a crystalline support (dealuminated Y zeolite), taking advantage of the near uniformity of its sites for bonding metal complexes. The complexes, formed by ion exchange with the precursors $RhCl_3$,[2] $RuCl_3$,[3] and $CuCl_2$,[4] were treated in O_2 at high temperatures to remove the chloride. The resultant rhodium nanoparticles were oxidatively fragmented with CO to give supported rhodium *gem*-dicarbonyls, which reacted with H_2 and with N_2 at 523 K to form rhodium complexes with CO and N_2 ligands. The sharpness of the infrared (IR) bands pointed to a high degree of structural uniformity of these anchored species.

A more precise synthesis of zeolite-supported metal complex involves a one-step reaction of an organometallic precursor [$Rh(C_2H_4)_2(acac)$ (acac = $CH_3COCHCOCH_3$)[5a] or *cis*-$Ru(acac)_2(\eta^2\text{-}C_2H_4)_2$[5b]] with the zeolite. Rhodium diethylene complexes on dealuminated Y zeolite were shown by temperature-dependent ^{13}C NMR spectroscopy to have a degree of dynamic uniformity unprecedented for supported species.[6] Because the ethylene ligands undergo facile conversions and the complexes are site-isolated, this supported complex opens the way to precise characterization of a family of related complexes in the absence of complications that characterize the solution chemistry: solvent effects[7] and metal−metal bond formation.[8,9] Precisely synthesized structures on zeolites, in contrast to those on oxides (the reactive sites of which are often defects or edge and corner sites[10]), can be determined with a precision unattainable for the nonuniform oxide-supported metal complexes−and an advantage of the uniform zeolitic species is that electronic structure calcula-

[†] University of California, Davis.
[‡] University of Alabama.
[§] University of Southern California.

(1) (a) Comas-Vives, A.; Gonzalez-Arellano, C.; Corma, A.; Iglesias, M.; Sanchez, F.; Ujaque, G. *J. Am. Chem. Soc.* **2006**, *128*, 4756. (b) Kervinen, K.; Bruijnincx, P. C. A.; Beale, A. M.; Mesu, J. G.; van Koten, G.; Klein Gebbink, R. J. M.; Weckhuysen, B. M. *J. Am. Chem. Soc.* **2006**, *128*, 3208. (c) Mukhopadhyay, K.; Sarkar, B. R.; Chaudhari, R. V. *J. Am. Chem. Soc.* **2002**, *124*, 9692. (d) Burk, M. J.; Gerlach, A.; Semmeril, D. *J. Org. Chem.* **2000**, *65*, 8933. (e) Lee, J.; Ishihara, A.; Dumeignil, F.; Qian, E. W.; Kabe, T. *J. Mol. Catal. A* **2004**, *213*, 207. (f) Ali, B. El.; Tijani, J.; Fettouhi, M.; El-Faer, M.; Al-Arfaj, A. *Appl. Catal., A* **2005**, *283*, 185.
(2) Miessner, H. *J. Am. Chem. Soc.* **1994**, *116*, 11522.
(3) (a) Miessner, H.; Richter, K. *Angew. Chem., Int. Ed.* **1998**, *37*, 117. (b) Miessner, H.; Richter, K. *J. Mol. Catal. A* **1999**, *146*, 107. (c) Landmesser, H.; Miessner, H. *J. Phys. Chem.* **1991**, *95*, 10544.
(4) Miessner, H.; Landmesser, H.; Jaeger, N.; Richter, K. *J. Chem. Soc., Faraday Trans.* **1997**, *93*, 3417.
(5) (a) Liang, A. J.; Bhirud, V. A.; Ehresmann, J. O.; Kletnieks, P. W.; Haw, J. F.; Gates, B. C. *J. Phys. Chem. B* **2005**, *109*, 24236. (b) Ogino, I.; Gates, B. C. *J. Am. Chem. Soc.* **2008**, *130*, 13338.

 10.1021/ja900041n CCC: $40.75

tions at the density functional theory (DFT) level can be used to verify spectroscopic assignments and resolve structures characterized by subtly different spectra.

Thus, zeolite-supported metal complexes offer the prospects of (a) surface chemistry determined with a rigor rivaling that attainable with molecular metal complexes in solution, but in the absence of the complications characteristic of solution chemistry, and (b), ultimately, blurring of the distinctions between homogeneous and surface reactions. We have now begun to realize these prospects in an investigation of reactions of zeolite-supported rhodium complexes. The reactants were (isotopically labeled) gas-phase compounds that form ligands on the rhodium, which were characterized with IR, ^{13}C NMR, and extended X-ray absorption fine structure (EXAFS) spectroscopies, guided by electronic structure calculations at the DFT level. The results include identification of heretofore unknown species, including an activated rhodium hydride complex.

Results

Structural Characterization of Initially Prepared Zeolite-Supported Rhodium Ethylene Complex. Data reported earlier characterize the zeolite-supported rhodium ethylene complex prepared by the reaction of $Rh(C_2H_4)_2(acac)$ with dealuminated zeolite Y.[5] EXAFS data show that (within error) each Rh atom was bonded on average to two ethylene ligands and to two oxygen atoms of the zeolite, in a structure represented schematically as follows (where the oxygen atoms are part of the zeolite lattice):[5]

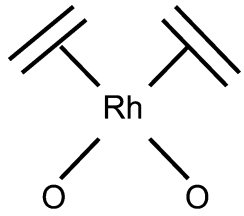

The IR spectrum of this sample in He (Figure 1a) includes bands in the C−H stretching region, between 2950 and 3100 cm^{-1} (Table 1), assigned to π-bonded ethylene[5] on the basis of a comparison of the spectrum with those of reference compounds such as $K[PtCl_3(C_2H_4)]$,[11] ethylene adsorbed on supported platinum particles, $Pt/\gamma\text{-}Al_2O_3$[12−14] and Pt/SiO_2,[15−19] as well as our DFT B3LYP/aug-cc-pVDZ and aug-cc-pVDZ-PP calculations (Table 1). The calculated frequencies show that there is very little interaction of the C_2H_4 groups with each other, as the calculated frequencies essentially occur in degenerate pairs

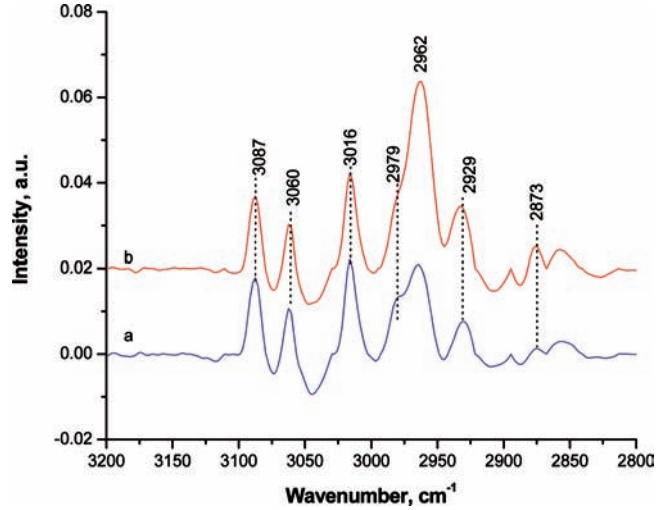

Figure 1. IR spectra in the C−H stretching region characterizing the sample formed by adsorption of $Rh(C_2H_4)_2(acac)$ on DAY zeolite. Data represent the sample after treatment in He (a) and 4% C_2H_4 in He for 60 min (b).

(although degeneracy is not required by symmetry; this result accounts in part for why only four bands are observed although eight are possible). Thus, the two ethylene sites are approximately symmetric.

Reaction of Supported Rhodium Ethylene Complex with C_2H_4 and with C_2D_4: Facile Ligand Exchange. Upon exposure of the supported rhodium diethylene complex to flowing ethylene, the intensities of the 2962- and 2929-cm^{-1} bands increased (Figure 1b) as new species formed (the spectrum represents the sample after removal of gas-phase ethylene).[20] These two bands are assigned to ethyl ligands, as the peak locations essentially match those of ethyl chloride,[21] ethyl groups adsorbed on Pt(111),[22] and our DFT calculations of the rhodium complexes containing the ethyl group: C_2H_5/H, C_2H_5/C_2H_5, and C_2H_4/C_2H_5 (Table 2). (On the basis of the calculations alone, we cannot confidently identify the other ligand present with the C_2H_5 group.)

EXAFS spectra were recorded as the supported rhodium diethylene sample was treated in ethylene at 298 K and atmospheric pressure in a cell that served as a flow reactor. EXAFS spectroscopy is not sensitive enough by itself to provide a sufficient characterization of all the changes in the sample, but the data are valuable in providing evidence (Figure 2; Table 3) showing (a) no indication of Rh−Rh contributions, consistent with mononuclear rhodium complexes and the lack of rhodium

(6) Ehresmann, J. O.; Kletnieks, P. W.; Liang, A.; Bhirud, V. A.; Bagatchenko, O. P.; Lee, E. J.; Klaric, M.; Gates, B. C.; Haw, J. F. *Angew. Chem., Int. Ed.* **2006**, *45*, 574.
(7) In contrast, anions in salts, such as chloride, are difficult to remove, although high-temperature treatment in H_2, for example, is sufficient, but it typically causes reduction and aggregation of the metal; Wovchko, E.; Yates, J. T., Jr. *J. Am. Chem. Soc.* **1996**, *118*, 10250.
(8) (a) Bonds, W. D., Jr.; Brubaker, C. H., Jr.; Chandrasekaran, E. S.; Gibbons, C.; Grubbs, R. H.; Kroll, L. C. *J. Am. Chem. Soc.* **1975**, *97*, 2128. (b) Liu, D. K.; Wrighton, M. S. *J. Am. Chem. Soc.* **1982**, *104*, 898.
(9) Kletnieks, P. W.; Liang, A. J.; Craciun, R.; Ehresmann, J. O.; Marcus, D. M.; Bhirud, V. A.; Klaric, M. M.; Hayman, M. J.; Guenther, D. R.; Bagatchenko, O. P.; Dixon, D. A.; Gates, B. C.; Haw, J. F. *Chem.−Eur. J.* **2007**, *13*, 7294.
(10) Hu, A.; Neyman, K. M.; Staufer, M.; Belling, T.; Gates, B. C.; Rösch, N. *J. Am. Chem. Soc.* **1999**, *121*, 4522.
(11) Hiraishi, H. *Spectrochim. Acta, Part A* **1969**, *25*, 749.
(12) Soma, Y. *J. Catal.* **1979**, *59*, 239.
(13) Mohsin, S. B.; Trenary, M.; Robota, H. J. *J. Phys. Chem.* **1991**, *95*, 6657.
(14) Mohsin, S. B.; Trenary, M.; Robota, H. J. *J. Phys. Chem.* **1988**, *92*, 5229.
(15) Chesters, M. A.; De La Cruz, C.; Gardner, P.; McCash, E. M.; Pudney, P.; Shahid, G.; Sheppard, N. *J. Chem. Soc., Faraday Trans.* **1990**, *86*, 2757.
(16) De La Cruz, C.; Sheppard, N. *Catal. Lett.* **1996**, *37*, 47.
(17) De La Cruz, C.; Sheppard, N. *J. Chem. Soc., Faraday Trans.* **1997**, *93*, 3569.
(18) Chesters, M. A.; De La Cruz, C.; Gardner, P.; McCash, E. M.; Prentice, J. D.; Sheppard, N. *J. Electron Spectrosc. Relat. Phenom.* **1990**, *54/55*, 739.
(19) De La Cruz, C.; Sheppard, N. *J. Chem. Soc., Faraday Trans.* **1997**, *93*, 3569.
(20) Transient data are not presented because the gas-phase ethylene interfered with the spectra of the supported species.
(21) Shimanouchi, T. *Natl. Stand. Ref. Data Ser. (US Natl. Bur. Stand.)* **1967**, *1*, 39. Table of Molecular Vibrational Frequencies.
(22) Hoffmann, H.; Griffiths, P. R.; Zaera, F. *Surf. Sci.* **1992**, *262*, 141.

Table 1. Vibrational Frequencies (ν, cm^{-1}) of the C−H(D) and C=C bonds in the C_2H_4 (and/or C_2D_4) Ligands Formed by Adsorption of $Rh(C_2H_4)_2(acac)$ on Dealuminated Y Zeolite[a]

ligands on Rh	mode assignment	ν characteristic of rhodium complex supported on DAY zeolite[b]	ν characteristic of rhodium complex supported on Al_2O_3[c]	ν characteristic of ethylene adsorbed platinum particles supported on Al_2O_3[d]	ν characteristic of ethylene adsorbed on platinum particles supported on SiO_2[e]	ν characteristic of rhodium complex supported on DAY zeolite calculated by DFT[b]
C_2H_4/C_2H_4	C−H	3084	3080	3073	3095	3090 (2)
C_2H_4/C_2H_4	C−H	3062		3018	3070	3062 (2)
C_2H_4/C_2H_4	C−H	3016		2998	3011	3002 (2)
C_2H_4/C_2H_4	C−H	2979	2966	2955	2980	2990 (2)
C_2H_4/C_2H_4	C=C/$\delta(CH_2)$	1440		1498	1616	1499
C_2H_4/C_2H_4	C=C/$\delta(CH_2)$			1200	1443	1488
C_2H_4/C_2H_4	C=C/$\delta(CH_2)$				1340	1216
C_2H_4/C_2H_4	C=C/$\delta(CH_2)$					1203
C_2D_4/C_2D_4	C−D	2321		2310		2318 (2)
C_2D_4/C_2D_4	C−D	2253				2301 (2)
C_2D_4/C_2D_4	C−D	2223		2213	2202	2214 (2)
C_2D_4/C_2D_4	C−D					2180 (2)
C_2D_4/C_2D_4	C=C					1325
C_2D_4/C_2D_4	C=C					1319
C_2D_4/C_2H_4	C−H					3090
C_2D_4/C_2H_4	C−H	3035		2914[d,e,f]		3065
C_2D_4/C_2H_4	C−H					3002
C_2D_4/C_2H_4	C−H					2990
C_2D_4/C_2H_4	C−D					2318
C_2D_4/C_2H_4	C−D					2301
C_2D_4/C_2H_4	C−D	2201		2079		2214
C_2D_4/C_2H_4	C−D					2180

[a] Values characterizing comparable structures are also shown. [b] This work. [c] Reference 13. [d] Reference 14. [e] Reference 17. [f] Niemantsverdriet, J. W. *Spectroscopy in Catalysis: An Introduction*; Wiley-VCH: Weinheim, 2000; p 203.

Table 2. C−H(D) Vibrational Frequencies (ν, cm^{-1}) of C_2H_5 (and/or C_2D_5) Ligands Formed by Adsorption of $Rh(C_2H_4)_2(acac)$ on Dealuminated Y Zeolite

method	ligands	ν_1	ν_2	ν_3	ν_4	ν_5	ν_6	ν_7	ν_8	ν_9	ν_{10}
expt	C_2H_5/R				2962	2943	2927				
DFT	C_2H_5/C_2H_5	3001	2975	2965	2958	2944	2930	2897	2891	2845	2826
DFT	C_2H_5/H		2979	2956		2939		2892			2772
DFT	C_2H_5/C_2H_4		2982		2955		2934	2897		2847	
DFT	C_2H_5/N_2		2980	2957		2947		2904	2891		
DFT	C_2H_5/CO	2995	2979		2957			2903		2843	
expt	C_2D_5/R	2237		2199							
DFT	C_2D_5/C_2D_5	2228	2207	2196	2190	2181	2172	2090	2084	2074	2062
DFT	C_2D_5/D		2209		2186	2178			2082		2026
DFT	C_2D_5/C_2D_4				2189	2178	2175	2089		2075	
DFT	C_2D_5/N_2		2212		2198	2181	2153	2112			
DFT	C_2D_5/CO	2220	2207		2191			2094		2077	

clusters; (b) a Rh−O contribution indicating that each Rh atom remained bonded to approximately two oxygen atoms of the support, on average; and (c) a Rh−C contribution indicating that each Rh atom was bonded to approximately three carbon atoms, in contrast to the initial value of four. The latter result is significant in indicating the presence of a carbon-containing ligand such as an alkyl in addition to a C_2H_4 ligand in the coordination sphere of the Rh; this point is addressed further below.

Further evidence of these changes emerged from experiments carried out with C_2D_4. Figure 2 shows IR spectra in the C−H stretching region recorded as pulses of C_2D_4 flowed through the cell containing the supported rhodium diethylene complex. Upon injection of a C_2D_4 pulse at 298 K and 1 bar (with the number of C_2D_4 molecules being slightly greater than the number of C_2H_4 ligands initially bonded to the rhodium), the four IR bands associated with the ethylene ligands (in the range of 2979−3084 cm^{-1}) were removed (Figure 3A, spectra b and c). Simultaneously, a band at 1440 cm^{-1}, indicative of the C=C stretch of a π-bonded ethylene species, also disappeared (data not shown). Four new IR bands appeared, between 2321 and 2188 cm^{-1} (Figure 3B, spectra b and c), that are assigned to deuterated ethylene species, essentially matching (a) those observed for π-bonded C_2D_4 in $K[PtCl_3(C_2D_4)]$;[11] (b) surface species formed by adsorption of C_2D_4 on Pt/γ-Al_2O_3[14] and Pt/SiO_2;[17] and (c) our DFT calculations for the isotopically substituted species.

In summary, the results indicate that the ethylene ligands on the supported rhodium complex underwent rapid exchange with C_2D_4 ligands in the gas phase. Additional new bands, at 3035 and 2201 cm^{-1} (Table 1), appeared in the IR spectrum during the ligand exchange (Figure 3, A and B, spectrum c); the assignment of these bands is given below.

After the replacement of C_2H_4 ligands with C_2D_4, the sample was treated with a pulse of C_2H_4; the results (Figure 3) show that the ligand exchange was reversible. All this evidence of the lability of the ethylene ligands is consistent with ^{13}C NMR spectra reported earlier.[9]

The transient data provide evidence of intermediates in the ligand-exchange process. A sharp band (fwhm 3 cm^{-1}) appeared at 2989 cm^{-1} as C_2H_4 was brought in contact with the sample containing C_2D_4 ligands (Figure 3A, spectrum d). This band

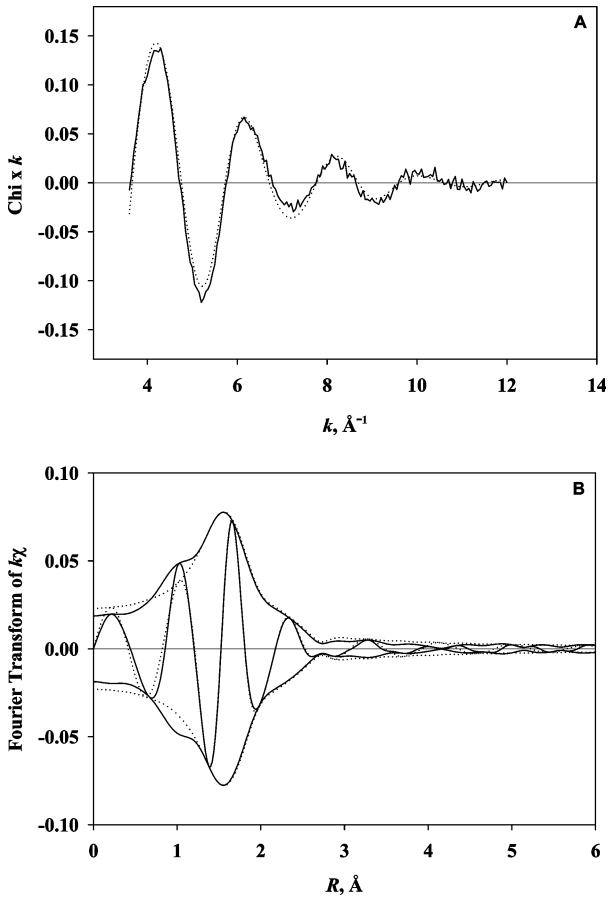

Figure 2. Results of EXAFS analysis characterizing the sample formed from $Rh(C_2H_4)_2(acac)$ and zeolite DAY subjected to C_2H_4 flow for 80 min at 298 K: (A) experimental EXAFS (χ) function (solid line), k^1 weighting and the sum of the calculated contributions (dotted line); (B) imaginary part and magnitude of uncorrected Fourier transform (k^1 weighted, Δk = 3.6−12.1 $Å^{-1}$) of experimental EXAFS (solid line) and sum of the calculated contributions (dotted line).

Table 3. EXAFS Results at the Rh K Edge Characterizing the Zeolite DAY-Supported Rhodium Complex during C_2H_4 Treatment[a]

absorber−backscatterer pair	*N*	*R* (Å)	$10^3 \times \Delta\sigma^2$ (Å^2)	ΔE_0 (eV)
Rh−Rh	—[b]			
Rh−O	2.1	2.06	4.9	2.4
Rh−C	2.9	2.20	6.8	2.4
Rh−Al[c]	0.6	3.06	8.6	0.8

[a] The accuracies of these parameters are estimated to be as follows (with the exception of the Rh−Al contribution): coordination number *N*, ±20%; distance *R*, ±0.02 Å; Debye−Waller factor $\Delta\sigma^2$, ±20%; and inner potential correction ΔE_0, ±20%. [b] Contribution not detectable. [c] The interpretation of the Rh−Al contribution characterizing the sample after ethylene treatment is tempered by the small coordination number; the uncertainty in the parameters characterizing the Rh−Al contribution is large as a consequence of the small coordination number and therefore not well established.

was evident during the first 6 min after injection of the C_2H_4 pulse (Figure 2d), but not later, and, during the 6-min period, the band shifted to 2979 cm^{-1} (Table 1). As shown in Table 1, the DFT calculations show that there should only be small changes in the frequencies as the mixed C_2H_4/C_2D_4 complex formed, and so we assign the 2989-cm^{-1} band to a C−H stretch of a π-bonded C_2H_4 ligand in the presence of a C_2D_4 ligand on Rh.

The bands at 3035 and 2201 cm^{-1} are assigned to rhodium complexes with a C_2H_4 and a C_2D_4 ligand ($Rh(C_2H_4)(C_2D_4)$),

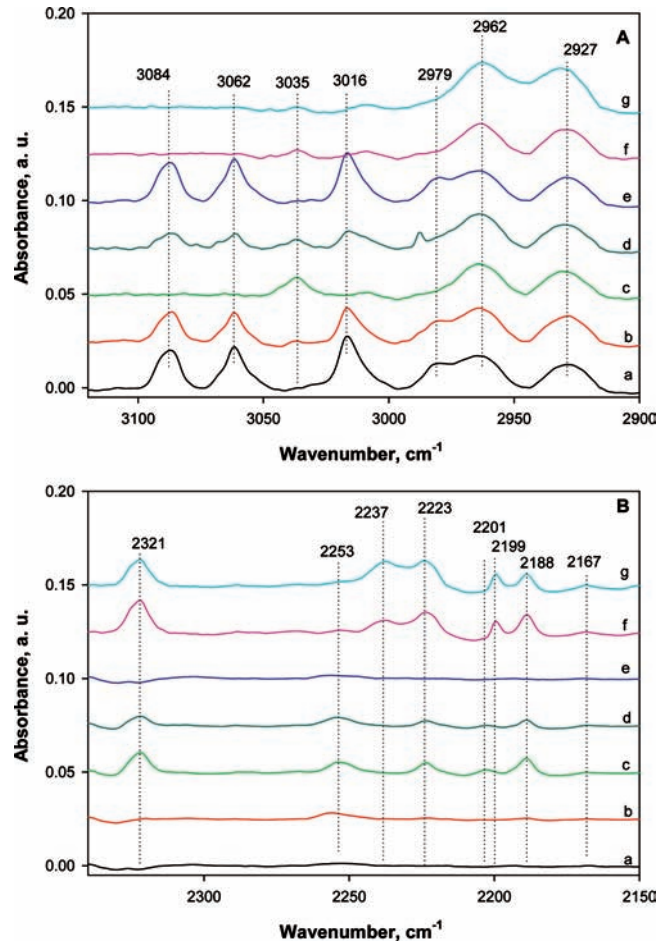

Figure 3. Temporal evolution of IR spectra. (A) Spectra in the C−H stretching region characterizing the sample formed by adsorption of $Rh(C_2H_4)_2(acac)$ on DAY zeolite after the following treatments, listed in sequence: (a) He, (b) C_2D_4 for 2 min, (c) C_2D_4 for 30 min, (d) C_2H_4 for 2 min, (e) C_2H_4 for 20 min, (f) C_2D_4 again for 12 min, and (g) C_2D_4 for 20 min. (B) IR spectra in the 2350−2150 cm^{-1} region of the sample formed by adsorption of $Rh(C_2H_4)_2(acac)$ and DAY zeolite treated in the same sequence of those listed in A: (a) He, (b) C_2D_4 for 2 min, (c) C_2D_4 for 30 min, (d) C_2H_4 for 2 min, (e) C_2H_4 for 20 min, (f) C_2D_4 again for 12 min, and (g) C_2D_4 for 20 min.

as these bands also disappeared when an excess of C_2D_4 reacted with the sample containing both ligands. Following the sequence of pulses of C_2D_4, then C_2H_4, and then C_2D_4, additional changes in the spectrum in both the C−H stretching and C−D stretching regions were observed (Figure 3, spectra f and g). During the final pulse, the intensities of the 2962- and 2927-cm^{-1} (Table 2) bands increased, and the 2927-cm^{-1} band was blue-shifted to 2943 cm^{-1} (Table 2 and Figure 3A, spectra f and g).

The new bands at 2962 and 2927 cm^{-1} clearly should not be assigned to C_2H_4; on the basis of our new DFT results (Table 2), they are assigned to ethyl groups. The shift of the latter is clearly associated with changes in the ligands coordinated to the Rh.

Further evidence of the formation of ethyl groups during the ligand exchange processes is provided by the observation of new IR bands at 2237 and 2199 cm^{-1} (Table 2) in the deuterated sample, which can be assigned to C_2D_5 ligands on the basis of our DFT results (Table 2) characterizing the isotopic shifts. The bands shifted from 2253 and 2201 cm^{-1} (Table 1) as their intensities increased, as was observed during the first pulse of C_2D_4. These bands are assigned to C_2D_5 complexed to Rh.

Table 4. Vibrational Frequencies (ν, cm^{-1}) of ^{12}CO (and/or ^{13}CO) Ligands Formed by Reaction of ^{12}CO (and/or ^{13}CO) with Supported Species formed by Adsorption of $Rh(C_2H_4)_2(acac)$ on Dealuminated Y Zeolite

method	ligands	$\nu_1(^{12}CO)$	$\nu_2(^{12}CO)$	$\nu_1(^{13}CO)$	$\nu_2(^{13}CO)$
DFT	CO/CO	2104	2041	2055	1994
expt	CO/CO	2117	2052	2068	2006
DFT	CO/N_2	2056		2007	
expt	CO/N_2	2062			
DFT	CO/H_2	2059		2010	
DFT	CO/C_2H_4	2037		1989	
DFT	CO/H	2080		2030	
DFT	CO/C_2H_5	2061		2012	

Thus, our results show that some of the π-bonded ethylene ligands were converted to ethyl during the ligand exchange. This reaction can be explained by the involvement of hydroxyl groups of the support in a process called reverse spillover.[23] Of interest is the nature of the ligands bonded to the rhodium when the ethyl group is formed. For the case of the C_2H_5 ligand, we cannot distinguish between the ligand pairs C_2H_5/C_2H_5, C_2H_5/H, and C_2H_5/C_2H_4 on the basis of a comparison of the calculated frequencies with the experimental values. However, for the C_2D_5 ligand, the calculated frequencies best match experiment if both ligands are C_2D_5. We emphasize that the structure of the species with two C_2H_5 ligands is asymmetric, with the two C_2H_5 ligands occupying inequivalent sites, a conclusion drawn on the basis of our calculations and the observed spectra.

Additional bands at 2756, 2677, and 2631 cm^{-1} were also observed when the sample was exposed to the final C_2D_4 pulse. These bands are assigned to isolated zeolite surface OD groups on the basis of spectra reported for hydroxylated zeolites.[24] The ratios of the frequencies of the 2756-, 2677-, and 2631-cm^{-1} OD bands to the corresponding OH bands are 0.73, 0.74, and 0.73, respectively. We also calculated the O−H and O−D stretching frequencies for a model of these species on the surface, $(SiH_3)_3Si(OH/OD)$, and predicted frequencies of 3730 and 2750 cm^{-1}, respectively (taking the scale factor from H_2O). The calculated O−D stretching frequency is in excellent agreement with the observed value of 2756 cm^{-1}, confirming the assignment. The observation of the O−D stretches suggests a hydrogen spillover process consistent with our preceding inference of reverse hydrogen spillover, which is well-known for metal oxides and zeolites incorporating supported transition metals.

Reaction of Supported Rhodium Ethylene Complex with CO. When a steadily flowing stream of 0.3 mol % CO in helium was brought in contact with the supported rhodium diethylene complex at 298 K and atmospheric pressure, rhodium *gem*-carbonyl species formed rapidly, as shown by two IR bands, at 2052 and 2117 cm^{-1}, assigned to ν_{CO}, consistent with our previous results,[5a] those of Miessner,[25] and the DFT calculations (Table 4). The frequencies essentially match those observed by Goellner et al.[26] for a zeolite-supported sample formed directly from $Rh(CO)_2(acac)$. These bands are narrow, with the fwhm of each being <6 cm^{-1}, indicating a high degree of uniformity

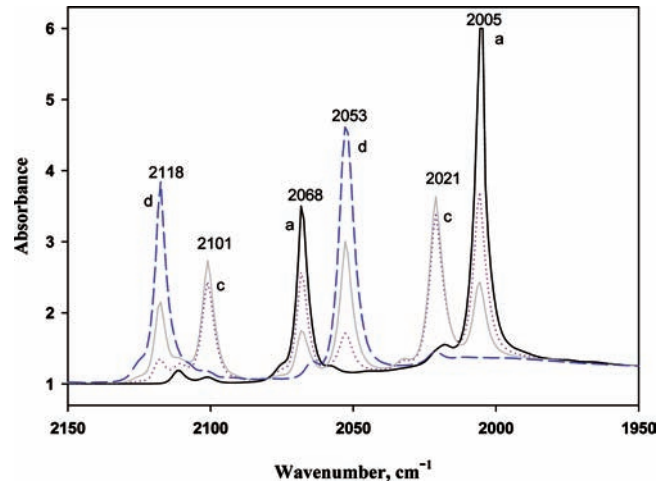

Figure 4. IR spectra in carbonyl stretching region characterizing the sample formed from $Rh(C_2H_4)_2(acac)$ and dealuminated Y zeolite after the sample was treated in flowing gases in the following sequence: (1) $1\%H_2$/He for 25 min, (2) a pulse of ^{13}CO in He, and then (3) 0.3% CO in He (sample was purged with He for 30 min before being brought in contact with CO) for (a) 0 min, (b) 6 min, (c) 8 min, and (d) 35 min.

of the supported rhodium complexes.[5a,25,26] Two satellite bands, at 2101 and 2021 cm^{-1}, were also observed, essentially matching earlier results.[25] The angle between the two metal−CO bonds can be estimated from the expression $I_s/I_{as} = \cot^2(\alpha/2)$, where I_s and I_{as} are the intensities of the symmetric and asymmetric stretching bands of CO, respectively, and α is the bond angle. The value of α is 106°,[28] consistent with the earlier results and somewhat larger than the value of 90.0° obtained in our DFT geometry optimizations.[5a]

Exchange of Rhodium Diethylene Complex with ^{13}CO. When a pulse of ^{13}CO in He was brought in contact with the sample, the four IR bands associated with the ethylene ligands disappeared (Figure 4a), and two new bands appeared, at 2068 and 2006 cm^{-1}. These two bands are assigned to the symmetric and asymmetric coupling of the ^{13}CO stretching vibrations of $Rh(^{13}CO)_2$, consistent with the DFT results (Table 4). The replacement of ethylene ligands by ^{13}CO was complete, and the exchange was so fast that we observed no evidence of intermediates.

Exchange of Rhodium ^{13}CO Complex with CO. When a continuous stream of 0.3 mol % CO in helium was brought in contact with the sample in which the ethylene ligands had been exchanged with ^{13}CO, the IR spectra (Figure 4b) show that the two ν_{CO} bands shifted to 2118 and 2053 cm^{-1}, matching the values observed for $Rh(^{12}CO)_2$; the spectra are characterized by isosbestic points at 2028 and 2078 cm^{-1} (Figure 4). During the transformation, bands were also observed at 2101 and 2021 cm^{-1}, and these are assigned to $Rh(^{13}CO)(^{12}CO)$ species, consistent with the assignment of the satellite peaks mentioned above and the DFT values of 2088 and 2009 cm^{-1} for the mixed complex.

Reaction of Supported Rhodium Dicarbonyl Complex with C_2H_4. When the supported rhodium dicarbonyl was brought in contact with a continuous stream of 60% C_2H_4 in helium, changes were observed in the ν_{CO} region (Figure 5). The asymmetric CO stretching band at 2118 cm^{-1} diminished in intensity, disappearing after 5 min. The symmetric CO stretching band at 2052 cm^{-1} was blue-shifted 4 cm^{-1} to 2056 cm^{-1}, and

(23) Kondo, J.; Domen, K.; Maruyak, K.; Onishi, T. *J. Chem. Soc., Faraday Trans.* **1990**, *86*, 3021.
(24) Domen, K.; Fujino, T.; Wada, A.; Hirose, C.; Kano, S. S. *Surf. Sci.* **1997**, *386*, 78.
(25) Miessner, H.; Burkhardt, I.; Gutschick, D.; Zecchina, A.; Morterra, C.; Spoto, G. *J. Chem. Soc., Faraday Trans. I* **1989**, *85*, 2113.
(26) Goellner, J. F.; Gates, B. C.; Vayssilov, G. N.; Rösch, N. *J. Am. Chem. Soc.* **2000**, *122*, 8056.
(27) Wang, X. F.; Andrews, L. *J. Phys. Chem. A* **2002**, *106*, 3706.

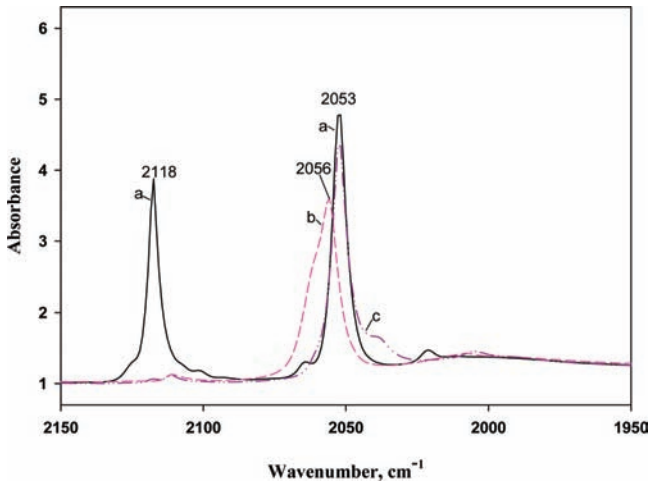

Figure 5. IR spectra in carbonyl stretching region characterizing the sample formed from $Rh(C_2H_4)_2(acac)$ and dealuminated Y zeolite that had been treated in flowing gases in the following sequence: (a) 0.3% CO in He, (b) 40% C_2H_4 in He (sample was evacuated for 5 min before being brought in contact with C_2H_4), and (c) He (after evacuation of gas-phase C_2H_4).

its bandwidth (fwhm) increased from 6 to 18 cm^{-1}, suggesting changes in the environment of the supported complex. The slight blue-shift suggests that ligands other than CO were bonded to the Rh centers (resulting in a weakening of the Rh−CO bond (Figure 5b)), and the increased bandwidth suggests a mixture of species. The disappearance of one CO band implies that C_2H_4 displaced the CO from the Rh. The calculations predict a slight red-shift of 4 cm^{-1} on binding of CO to the complex with C_2H_4.

Upon subsequent evacuation of the sample, the symmetric ν_{CO} band shifted back to its original position at 2052 cm^{-1}, with the bandwidth attaining the previous value of 6 cm^{-1} (Figure 5c), suggesting that the ethylene had desorbed from the rhodium centers. (Only one ν_{CO} peak was observed after evacuation.)

Mass Spectrometry Evidence of Changes in the Ligands on Rhodium. Mass spectra of the effluent gases were recorded during the previously described flow experiments. The mass spectra demonstrate the presence of gas-phase products, providing additional evidence of changes in the ligand environment of the rhodium.

Figure 6 shows mass spectra of the effluent gases when the supported rhodium diethylene complex was treated at 298 K and atmospheric pressure with the following sequence of gases, each flowing continuously: helium, ethylene, helium, CO, helium, ethylene, helium, and then CO. When the sample was initially brought in contact with helium, no change was observed in the mass spectra. Subsequent exposure to ethylene led to the observation of no gas-phase components other than ethylene itself (m/e = 28, 27, and 26). The system was then purged with helium, and the end of the purge was demonstrated by the lack of ethylene detected by mass spectrometry. Then the sample was exposed to flowing CO, and ethylene (characterized by m/e = 26, 27, and 28, Figure 6, inset) appeared and, within 5 min, disappeared, indicating that CO had displaced ethylene from the Rh and that ethylene was rapidly purged. These observations are consistent with the IR results demonstrating the formation of rhodium dicarbonyl complexes.

Contacting of this sample with C_2H_4, after purging traces of CO from the system, led to a period during which there were no informative changes in the mass spectra (both ethylene and CO are characterized by m/e = 28). Nonetheless, structural changes in the supported rhodium complex were occurring, as evidenced by changes in the IR spectra, which show that one of the bands associated with CO ligands (2118 cm^{-1}) disappeared after the supported rhodium dicarbonyl had been exposed to ethylene. The results are consistent with the suggestion that ethylene replaced one of the CO ligands on each Rh atom.

When the sample was subsequently exposed again to flowing CO after 1 h in flowing C_2H_4, changes in the mass numbers associated with C_2H_4, similar to those mentioned above, became evident; signals at m/e = 26, 27, and 28 appeared and then disappeared within minutes after the start of CO flow (Figure 6, inset). These results show that ethylene displaced CO from the rhodium.

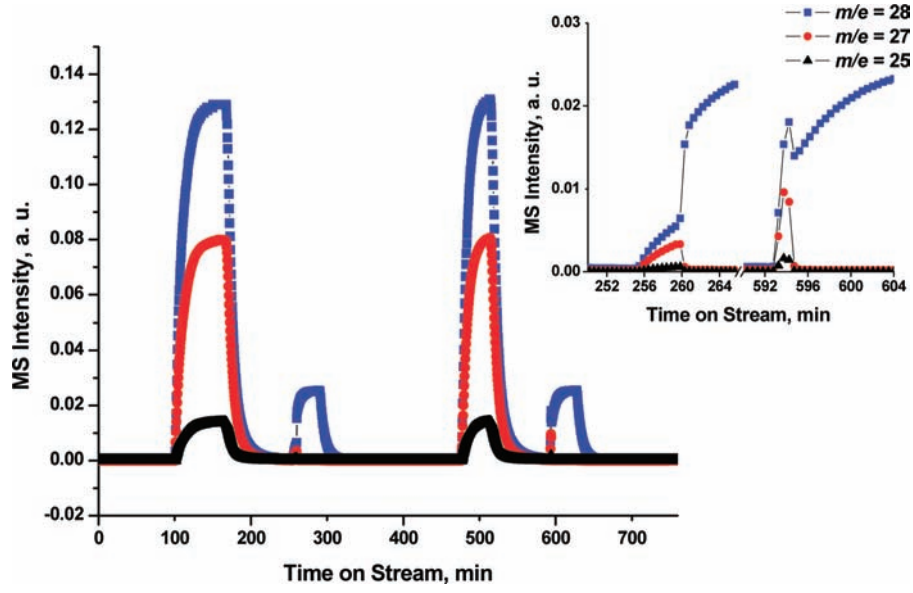

Figure 6. Mass spectra characterizing the effluent gas after the zeolite-supported rhodium complex had been treated in flowing gases in the following sequence: (1) ethylene (m/e = 25, 27, and 28) for 90 min; then (2) purged with He for 60 min; (3) CO (m/e = 28) for 60 min, and then (4) purged with He for 180 min. The same flow sequence was repeated once more (the sample being in contact with ethylene for 60 min first and then purged with He for 60 min, and finally being in contact with CO for 60 min).

Table 5. Vibrational Frequencies (ν, cm^{-1}) of Rh−H (and/or Rh-D) Formed by Reaction of H_2 and/or D_2 with Species Formed by Adsorption of $Rh(C_2H_4)_2(acac)$ on Dealuminated Y Zeolite

method	ligands	ν_1	ν_2
DFT	H/CO	2092	
expt	H/CO	2092	
DFT	H_2	2213	2182
DFT	H/N_2	2089	
DFT	H/C_2H_4	2103	
DFT	H/C_2H_5	2219	
DFT	D/CO	1486	
expt	D/CO	1486	
DFT	D_2	1574	1550
DFT	D/N_2	1485	
DFT	D/C_2D_4	1494	
DFT	D/C_2D_5	1578	

Table 6. DFT Vibrational Frequencies (ν, cm^{-1}) of Rh−H (and/or Rh−D) Characterizing Molecular Hydrogen (H_2) Bonded to Rh in the Zeolite-Supported Metal Complex

ligands	ν_1	ν_2
H_2/CO	2314	2015
H_2/N_2	2326	2002
H_2/C_2H_4	2396	2008
H_2/C_2H_5	2657	1867
D_2/CO	1642	1428
D_2/N_2	1650	1419
D_2/C_2D_4	1700	1423
D_2/C_2D_5	1882	1322

Reaction of Supported Rhodium Ethylene Complex with H_2. Upon exposure of the supported rhodium diethylene complex to a stream of 4% H_2 in helium, hydrogenation of the ethylene ligands occurred, forming ethane, detected by mass spectrometry, consistent with earlier results[5a] and with catalysis of ethylene hydrogenation by the rhodium complex.[5a]

IR spectra of the sample in H_2 show that new bands in the carbonyl stretching region appeared as the bands associated with ethylene ligands disappeared. A weak, sharp band grew in at 2092 cm^{-1} (Table 5). This band could be assigned to a rhodium hydride,[27] a rhodium carbonyl, or a combination of the two.[28] To test the hypothesis that the 2092-cm^{-1} band should be assigned to a rhodium hydride, a pulse of D_2 in flowing helium was injected at 298 K. A new IR band grew in at 1486 cm^{-1} in addition to the one at 2092 cm^{-1}. The new band matches that of supported labeled metal−deuteride species[29,31] (Supporting Information) as well as the DFT results discussed below. The ratio of the frequencies (2092 and 1486 cm^{-1}) is consistent with the replacement of H by D.

The calculated results (Table 5) clearly indicate the presence of a rhodium monohydride. Rhodium dihydrides are ruled out because the predicted dihydride frequency (Table 6) is clearly too high relative to the experimental range, and the dihydrides complexed with CO or N_2 yield peaks that are too high and too low in frequency, respectively. There is excellent agreement between experiment and calculation for the monohydride with a CO or a C_2H_4 also bonded to the Rh atom; we infer that C_2H_4 was present in the complex. However, we cannot rule out the possibility that CO could also have been present, which could potentially have been formed from surface acac ligands and H_2. (The predicted CO stretching frequency with the ligands being CO and H_2 is 2059 cm^{-1}, consistent with previous DFT calculations representing $Rh(CO)(H_2)$,[28] but the H_2 frequency is too high, and so we rule out this candidate assignment.)

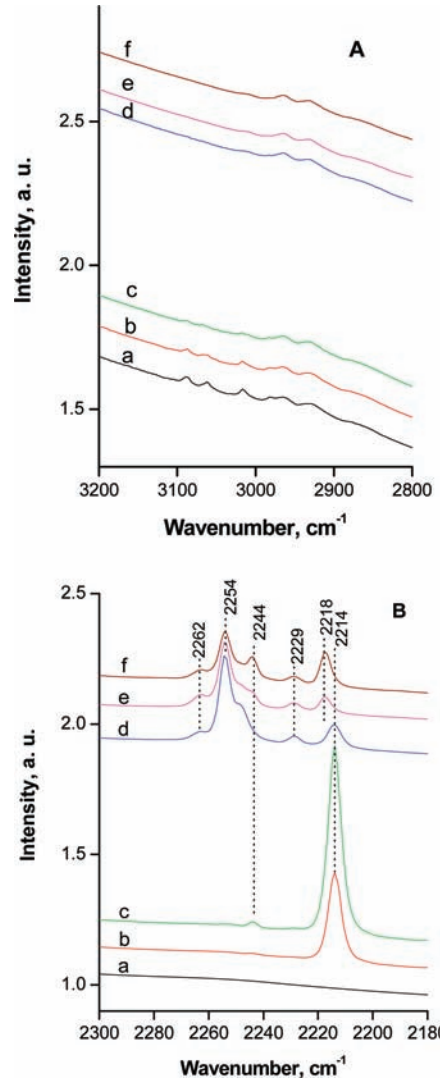

Figure 7. Temporal evolution of IR spectra. (A) C−H stretching region characterizing the sample formed from $Rh(C_2H_4)_2(acac)$ and dealuminated zeolite Y at 298 K and atmospheric pressure after contacting with a pulse of H_2 in N_2 for: (a) 0 min (N_2 only), (b) 2 min, (c) 4 min, and with subsequent pulses of H_2 for (d) 2 min, and then in N_2 only again for (e) 5 min and (f) 10 min. (B) N_2 and CO stretching regions characterizing the sample formed from $Rh(C_2H_4)_2(acac)$ and dealuminated zeolite Y at 298 K and atmospheric pressure after contacting with a pulse of H_2 in N_2 for: (a) 0 min (flow was N_2 only), (b) 2 min, (c) 4 min, and with subsequent pulses of H_2 for (d) 2 min, and then in N_2 only again for (e) 5 min and (f) 10 min.

In summary, the experimental and computational results strongly indicate that the band should be assigned to a rhodium monohydride species incorporating a C_2H_4 ligand, although we cannot completely rule out the possibility that some CO (which could have been formed from acac ligands and H_2) may have been present in place of the C_2H_4.

Other experiments with an isotopically labeled species (^{13}CO) were performed to test whether species other than hydride were bonded to the rhodium, but the data provided no definite answer regarding the assignment of the 2092-cm^{-1} band, because the intense rhodium *gem*-dicarbonyl bands (at 2067 and 2006 cm^{-1}) formed almost instantaneously upon contact of the sample with ^{13}CO.

(28) Vayssilov, G. N.; Rösch, N. *J. Am. Chem. Soc.* **2002**, *124*, 3783.
(29) Dixon, L. T.; Barth, R.; Gryder, J. W. *J. Catal.* **1975**, *37*, 368.

Table 7. Vibrational Frequencies (ν, cm^{-1}) of Isotopically Labeled N_2 Ligands in Rhodium Complexes Supported on Dealuminated Zeolite Y at 298 K

ligands	ν (experiment)	ν (DFT)[c]
$^{12}CO/^{14}N_2$	2254[a,b,c]	2226
$^{12}CO/^{15}N_2$	2177[a,c]	2152
$^{14}N_2/^{14}N_2$	2244, 2218[a,c]	2230, 2194
$^{15}N_2/^{15}N_2$	2168, 2144[a,c]	2153, 2120
$^{14}N_2/^{15}N_2$	2232, 2154[a,c]	2215, 2133
$^{14}N_2/C_2H_5$	2214[c]	2214
$^{15}N_2/C_2H_5$	2140[c]	2140
$^{14}N_2/H$		2230
$^{15}N_2/H$		2155
$^{14}N_2$	2214[c]	2212
$^{15}N_2$	2140[c]	2138
$^{14}N_2/H_2$		2209
$^{15}N_2/H_2$		2134
$^{14}N_2/C_2H_4$		2190
$^{15}N_2/C_2H_4$		2116

[a] Reference 2. [b] Reference 41 (2252 cm^{-1}). [c] This work.

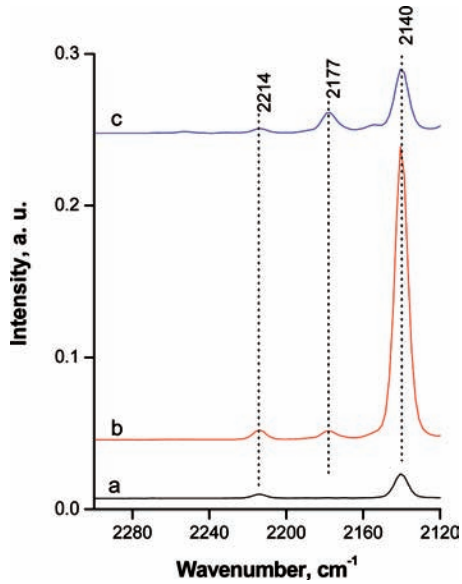

Figure 8. IR difference spectra of N_2 and CO stretching regions characterizing the sample formed from $Rh(C_2H_4)_2(acac)$ and dealuminated zeolite Y at 298 K and atmospheric pressure after contacting with a pulse of H_2 and $^{15}N_2$ in He for: (a) 2 min, (b) 8 min, and (c) 22 min. The IR spectrum of the initially prepared supported rhodium sample in He was used as a reference spectrum. The difference spectra were obtained by subtracting the reference spectrum from those observed when sample was in H_2, $^{15}N_2$, and He.

Reaction of Supported Rhodium Ethylene Complex in N_2 and H_2: Formation of Rhodium Complexes with Nitrogen Ligands. When the supported rhodium diethylene complex was exposed to flowing N_2 for 30 min at 298 K and atmospheric pressure, no changes were observed in the IR spectra (Figure 7), indicating that the sample was stable. However, when the sample was exposed to a pulse of H_2 in a stream of N_2 at 298 K, ethane was detected in the effluent by mass spectrometry, and the IR spectra showed changes in the C−H stretching region (Figure 7A). The intensities of the IR bands associated with ethylene ligands decreased, indicating their reaction with H_2, as confirmed by the mass spectra showing ethane in the effluent. Simultaneously, changes were observed in the N_2 stretching region of the IR spectra. A sharp new high-intensity band appeared at 2214 cm^{-1} (fwhm = 7 cm^{-1}, Figure 7B, spectra b and c; Table 7); its intensity increased and reached a maximum

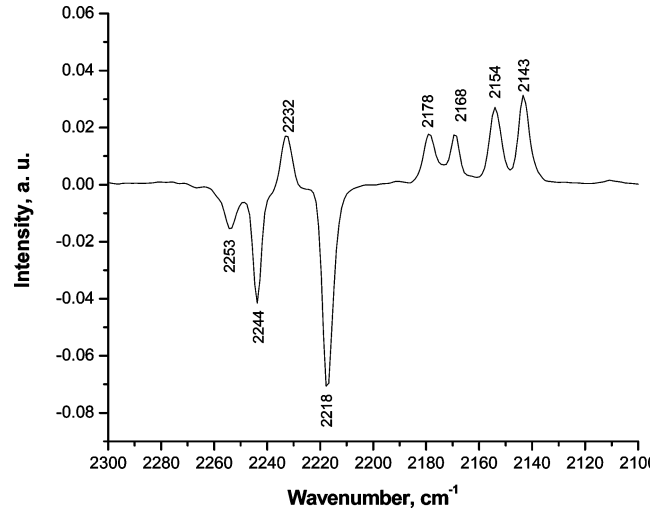

Figure 9. IR difference spectrum in N_2 stretching region characterizing the sample prepared from $Rh(C_2H_4)_2(acac)$ and DAY zeolite after the addition of a pulse of $^{15}N_2$ to a steadily flowing stream of $^{14}N_2$ at 298 K and atmospheric pressure flowing over the sample. The spectrum of the initially prepared sample, which was exposed to a pulse of H_2 in $^{14}N_2$ and followed by a continuously flowing stream of $^{14}N_2$, was used as a reference spectrum. The difference spectrum was obtained by subtracting the reference spectrum from the spectrum observed when a pulse of $^{15}N_2$ was in contact with the sample.

after 30 min of N_2 flow. When subsequent pulses of H_2 were injected into the N_2 stream, the intensity of the 2214-cm^{-1} band decreased, and a new band appeared at 2254 cm^{-1} (Table 7 and Figure 7B, spectrum d). The intensity of this band increased at the expense of the 2214-cm^{-1} band. The frequencies of these two bands fall in the range characteristic of dinitrogen ligands in metal complexes,[30] as well as dinitrogen adsorbed on single crystals of metal and on supported metal particles.[2,31−34]

Two other low-intensity bands, at 2262 and 2227 cm^{-1}, were observed in the N_2 stretching region and are attributed to new rhodium species with nitrogen ligands; the band assignments are discussed below. Simultaneous with the appearance of these bands, the bands associated with ethylene ligands disappeared.

Once traces of H_2 were no longer detected by mass spectrometry in the effluent and the sample was in contact only with flowing N_2, further changes were observed in the N_2 stretching region of the spectra. The band at 2214 cm^{-1} disappeared, and simultaneously two new bands grew in, at 2218 and 2244 cm^{-1} (Table 7 and Figure 7B, spectra e and f). Because these bands grew in proportion to each other, they are assigned to another nitrogen species.

DFT calculations were used to help assign these bands. We first investigated whether the bonding of N_2 is head-on (σ) or side-on (π). As expected, the bonding of two N_2 molecules to the Rh atom was found to be σ/σ, with the π/π structure being 30 kcal/mol less stable than the σ/σ structure. The frequencies corresponding to the π-bonded structures are also too low; we predict frequencies of 2046 and 2069 cm^{-1} for the π/π structure and 2230 and 2194 cm^{-1} for the σ/σ structure. Clearly, the experimental frequencies are consistent only with σ bonding; the $^{14}N_2/^{14}N_2$ calculated values of 2194 and 2230 cm^{-1} for the

(30) Morris, R. H. *Inorg. Chem.* **1992**, *31*, 1471.
(31) Pei, Z.; Fang, T. H.; Worley, S. D. *J. Phys. Chem.* **1995**, *99*, 3663.
(32) Wey, J. P.; Neely, W. C.; Worley, S. D. *J. Phys. Chem.* **1991**, *95*, 8879.
(33) Wovchko, E. A.; Yates, J. T., Jr. *J. Am. Chem. Soc.* **1996**, *118*, 10250.
(34) Wang, H. P.; Yates, J. T., Jr. *J. Phys. Chem.* **1984**, *88*, 852.

Table 8. Calculated Ligand Dissociation Energies in kcal/mol for $Al(OH)_4RhLL'$ and $Al(OH)_4RhL$ Complexes[a,b]

BDE1 reaction	BDE1	BDE2 reaction	BDE2	BDE1 + BDE2
$Rh(CO)_2 \rightarrow RhCO + CO$	54.1	$RhCO \rightarrow Rh + CO$	46.8	100.9
$Rh(C_2H_4)CO \rightarrow RhCO + C_2H_4$	42.6	$RhCO \rightarrow Rh + CO$	46.8	89.4
$Rh(C_2H_4)CO \rightarrow RhC_2H_4 + CO$	54.4	$RhC_2H_4 \rightarrow Rh + C_2H_4$	35.0	
$Rh(N_2)_2 \rightarrow RhN_2 + N_2$	27.0	$RhN_2 \rightarrow Rh + N_2$	23.4	50.4
$Rh(N_2)CO \rightarrow RhN_2 + CO$	51.5	$RhN_2 \rightarrow Rh + N_2$	23.4	74.8
$Rh(N_2)CO \rightarrow RhCO + N_2$	28.0	$RhCO \rightarrow Rh + CO$	46.8	
$Rh(N_2)H \rightarrow RhN_2 + H$	63.9	$RhN_2 \rightarrow Rh + N_2$	23.4	87.3
$Rh(N_2)H \rightarrow RhH + N_2$	31.6	$RhH \rightarrow Rh + H$	55.7	
$Rh(CO)H \rightarrow RhCO + H$	65.5	$RhCO \rightarrow Rh + CO$	46.8	112.3
$Rh(CO)H \rightarrow RhH + CO$	56.7	$RhH \rightarrow Rh + H$	55.7	
$Rh(CO)H_2 \rightarrow RhCO + H_2$	30.1	$RhCO \rightarrow Rh + CO$	46.8	76.9
$Rh(CO)H_2 \rightarrow RhH_2 + CO$	55.3	$RhH_2 \rightarrow Rh + H_2$	21.6	
$Rh(CO)H_2 \rightarrow Rh(CO)H + H$	65.4			
$Rh(C_2H_4)_2 \rightarrow RhC_2H_4 + C_2H_4$	38.0	$RhC_2H_4 \rightarrow Rh + C_2H_4$	35.0	73.0
$Rh(C_2H_4)N_2 \rightarrow RhC_2H_4 + N_2$	29.4	$RhC_2H_4 \rightarrow Rh + C_2H_4$	35.0	64.4
$Rh(C_2H_4)N_2 \rightarrow RhN_2 + C_2H_4$	41.1	$RhN_2 \rightarrow Rh + N_2$	23.4	
$Rh(C_2H_4)H \rightarrow RhC_2H_4 + H$	62.3	$RhC_2H_4 \rightarrow Rh + C_2H_4$	35.0	97.3
$Rh(C_2H_4)H \rightarrow RhH + C_2H_4$	41.7	$RhH \rightarrow Rh + H$	55.7	
$Rh(C_2H_4)H_2 \rightarrow RhC_2H_4 + H_2$	26.8	$RhC_2H_4 \rightarrow Rh + C_2H_4$	35.0	61.8
$Rh(C_2H_4)H_2 \rightarrow RhH_2 + C_2H_4$	40.2	$RhH_2 \rightarrow Rh + H_2$	21.6	
$Rh(C_2H_4)H_2 \rightarrow Rh(C_2H_4)H + H$	65.4			
$Rh(C_2H_4)C_2H_5 \rightarrow RhC_2H_4 + C_2H_5$	43.7	$RhC_2H_4 \rightarrow Rh + C_2H_4$	35.0	78.7
$Rh(C_2H_4)C_2H_5 \rightarrow RhC_2H_5 + C_2H_4$	34.9	$RhC_2H_5 \rightarrow Rh + C_2H_5$	43.9	
$Rh(C_2H_5)N_2 \rightarrow RhC_2H_5 + N_2$	24.2	$RhC_2H_5 \rightarrow Rh + C_2H_5$	43.9	68.1
$Rh(C_2H_5)N_2 \rightarrow RhN_2 + C_2H_5$	44.7	$RhN_2 \rightarrow Rh + N_2$	23.4	
$Rh(C_2H_5)H \rightarrow RhC_2H_5 + H$	59.8	$RhC_2H_5 \rightarrow Rh + C_2H_5$	43.9	103.7
$Rh(C_2H_5)H \rightarrow RhH + C_2H_5$	48.0	$RhH \rightarrow Rh + H$	55.7	
$Rh(C_2H_5)CO \rightarrow RhC_2H_5 + CO$	48.1	$RhC_2H_5 \rightarrow Rh + C_2H_5$	43.9	91.9
$Rh(C_2H_5)CO \rightarrow RhCO + C_2H_5$	45.1	$RhCO \rightarrow Rh + CO$	46.8	
$Rh(C_2H_5)_2 \rightarrow RhC_2H_5 + C_2H_5$	43.6	$RhC_2H_5 \rightarrow Rh + C_2H_5$	43.9	87.5
$Rh(C_2H_5)H_2 \rightarrow RhC_2H_5 + H_2$	21.6	$RhC_2H_5 \rightarrow Rh + C_2H_5$	43.9	65.4
$Rh(C_2H_5)H_2 \rightarrow RhH_2 + C_2H_5$	43.8	$RhH_2 \rightarrow Rh + H_2$	21.6	
$Rh(C_2H_5)H_2 \rightarrow Rh(C_2H_5)H + H$	62.6			
$Rh(N_2)H_2 \rightarrow RhN_2 + H_2$	27.7	$RhN_2 \rightarrow Rh + N_2$	23.4	51.1
$Rh(N_2)H_2 \rightarrow RhH_2 + N_2$	29.4	$RhH_2 \rightarrow Rh + H_2$	21.6	
$Rh(N_2)H_2 \rightarrow Rh(N_2)H + H$	64.7			
$RhH_2 \rightarrow RhH + H$	66.8	$RhH \rightarrow Rh + H$	55.7	
$RhH_2 \rightarrow Rh + H_2$	21.6			

[a] The $Al(OH)_4$ is not shown. [b] All species are singlets except for $Rh = Al(OH)_4Rh$ and $RhN_2 = Al(OH)_4RhN_2$, which are triplets. $RhH = Al(OH)_4RhH$ and $RhC_2H_5 = Al(OH)_4\ RhC_2H_5$ are doublets. The singlet−triplet splitting in $Rh = Al(OH)_4Rh$ is 10.5 kcal/mol, and the singlet−triplet splitting in $RhN_2 = Al(OH)_4RhN_2$ is 1.4 kcal/mol. The ligand dissociation energies will increase if the higher energy state is assumed.

σ/σ structure are in good agreement with the experimental values of 2218 and 2244 cm^{-1}. Furthermore, the peak at 2214 cm^{-1} is consistent with an assignment to a N_2/C_2H_5 species.

To provide more information about the identities of the species indicated by the new bands that appeared when the sample was first brought in contact with H_2 pulses in N_2 (and then in flowing N_2 alone), experiments were performed with $^{15}N_2$.[35] When a pulse of $^{15}N_2$ in flowing helium was injected, no changes were observed in the spectrum, consistent with the observations with $^{14}N_2$ pulses.

However, when a pulse of $^{15}N_2$ mixed with H_2 was injected into the stream of continuously flowing helium, difference IR spectra (Figure 8) indicated the bonding of nitrogen to the rhodium at 298 K and atmospheric pressure. A sharp, intense band at 2140 cm^{-1} was observed immediately (Table 7 and Figures 8a and b); this is assigned to a rhodium complex with a $^{15}N_2$ ligand, with C_2H_5 being the other ligand. Another (weak) band, observed at 2214 cm^{-1} and mentioned above, is assigned to rhodium complexes with $^{14}N_2$ ligands (formed from the 2% $^{14}N_2$ impurity in $^{15}N_2$). A new band at 2177 cm^{-1} (Table 7 and Figure 8b and c) also appeared 8 min after injection of the pulse of $^{15}N_2 + H_2$. This band is assigned to dinitrogen species containing $^{15}N_2$, as discussed below. The intensity of the 2177-cm^{-1} band increased as the intensity of the 2140-cm^{-1} band decreased.

Two other (weak) bands associated with nitrogen species were observed. Consistent with the low intensities of these bands at 2262 and 2227 cm^{-1} that characterize the sample treated with a pulse of H_2 in $^{14}N_2$, bands associated with $^{15}N_2$ were not observed, and so it is inappropriate to assign these two bands to N_2 ligands.

A complementary isotopic tracer experiment was performed with N_2 instead of helium as the carrier gas. The changes in the spectra after exposure of the sample to a pulse of H_2 in $^{14}N_2$ and then to a pulse of $^{15}N_2$ in $^{14}N_2$ are shown in Figure 9. As expected, the bands characterizing the rhodium complex with $^{14}N_2$ ligands, at 2253, 2244, and 2218 cm^{-1}, decreased in intensity, and new bands characteristic of the rhodium complex incorporating $^{15}N_2$ ligands (at 2232, 2178, 2168, 2154, and 2143 cm^{-1}) appeared. Assignments of these bands are shown in Table 7. The calculated $^{15}N_2$ frequencies are in good agreement with the experimental values and confirm the assignments. It is possible that the bands at 2214 cm^{-1} for N_2 and 2140 cm^{-1} for $^{15}N_2$ could correspond to a single N_2 bonding to the Rh center.

Calculated Ligand Dissociation Energies. Ligand dissociation energies (LDEs) calculated for the supported rhodium complexes

(35) Attempts to record ^{15}N NMR spectra of the supported rhodium samples formed from $^{15}N_2$ were not successful. No rhodium dinitrogen species with $^{15}N_2$ were observed, and only peaks associated with gas-phase N_2 were evident in the spectrum.

Scheme 1

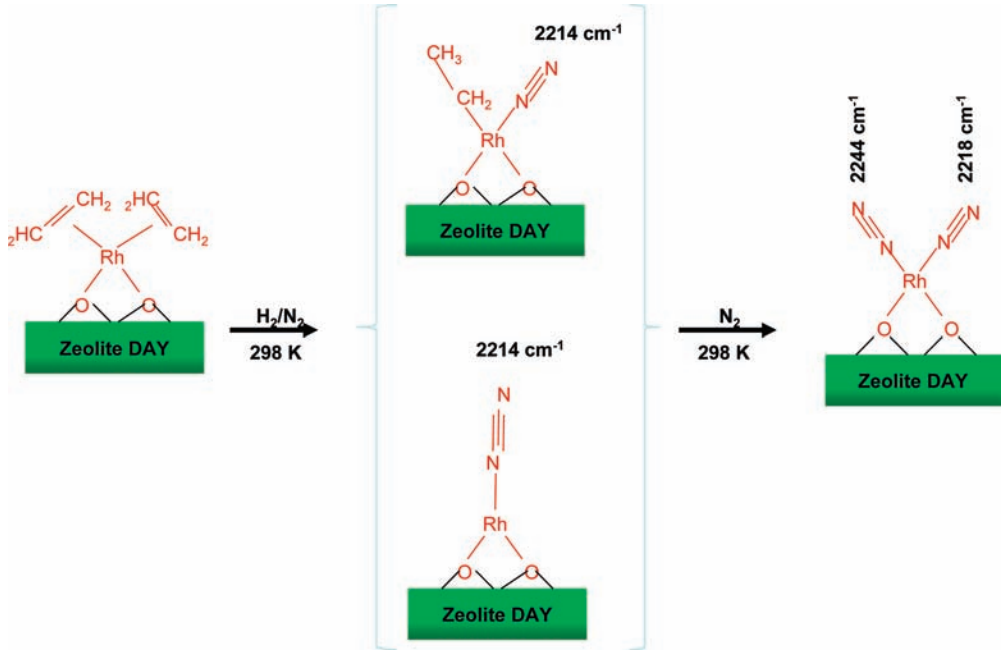

are summarized in Table 8. Although we do not expect the values to be accurate to better than ±5 kcal/mol at the current DFT level without benchmarking to more accurate methods (which was beyond the scope of this work), the relative energies should be accurate within a few kcal/mol.

For a complex zeolite-RhLL′ (two ligands bonded to Rh), we can predict the Rh−L ligand dissociation energy for any L. The average Rh−L dissociation energies (in kcal/mol) are as follows: $\Delta E(\mathrm{H}) = 64 > \Delta E(\mathrm{CO}) = 53 > \Delta E(\mathrm{C_2H_5}) = 45 > \Delta E(\mathrm{C_2H_4}) = 40 > \Delta E(\mathrm{N_2}) = 28 \approx \Delta E(\mathrm{H_2}) = 27$. These values are slightly higher than the ligand dissociation energies for the complex zeolite−Rh−L with a single ligand bonded to the Rh. Thus, we would expect CO to displace C_2H_4, for example, in an equilibrium situation. However, the results must be used carefully in any analysis of the exchange reactions in the flow experiments−which were carried out under conditions far from equilibrium−so that the treatments in the flow system could lead to endothermic exchange processes.

For comparison, we also calculated the LDEs for a single ligand binding to the Rh atom in the quartet state and to the Rh^+ ion in the triplet state (Supporting Information). These LDEs exhibit exactly the same trends for the Rh atom and the complex $Al(OH)_4Rh$, and the LDEs are of the same magnitude in each. The ordering changes somewhat for the LDEs of Rh^+, with C_2H_5 and C_2H_4 being the most strongly bound. These comparisons provide qualitative trends, and any comparisons need to be made carefully as the spin states can be different for the different species, and these can influence the LDEs. N_2 binds to the Rh in any of these species with about half the energy of the Rh−CO moiety in all three cases.

Discussion

Exchange of Ligands on Supported Rhodium Complex. An advantage of the zeolite-supported rhodium diethylene structure is the lability of the ethylene ligands, which is demonstrated clearly by our data. This metal complex allows facile examination of the chemistry in the ligand sphere of rhodium in the absence of solvents and at temperatures low enough that the rhodium species remain mononuclear. At higher temperatures (>298 K), the rhodium complex in the presence of H_2 is reduced and converted into clusters, as described elsewhere.[36]

Supported Rhodium Dinitrogen Complexes. Band Assignments. When the zeolite-supported rhodium ethylene complex was in contact with H_2, the ethylene ligands were hydrogenated to form ethane, which desorbed, as demonstrated by the effluent gas analyses. We infer that this facile removal of the ethylene ligands created coordinatively unsaturated Rh atoms that were bonded only to oxygen atoms of the support. Being site isolated, the coordinatively unsaturated Rh centers reacted even with N_2, giving rhodium complexes with a low Rh−ligand bond energy <30 kcal/mol.

We emphasize that, as formation of the rhodium dinitrogen species progressed, some ethylene ligands remained bonded to the rhodium, as evidenced by the IR bands in the C−H stretching region (Figure 7A, spectra b and c) and confirmed by the DFT calculations. Because the formal oxidation state of rhodium in the zeolite-supported $Rh(C_2H_4)_2$ was +1, the oxidation state of rhodium in the surface species is not expected to be different when nitrogen ligands are present. Although a relatively large number of transition metal complexes containing N_2 ligands are known,[30,37,38] only a few are known for supported metals[2−4,39,40]−most of them formed at low temperatures or high pressures. The finding that N_2 adsorbed on the zeolite-supported rhodium complex even at 298 K suggests new possibilities for catalysis by supported rhodium complexes.

During the sample treatments in N_2 when a small amount of H_2 was also present, a low-frequency mode at 2214 cm^{-1} appeared at the beginning of the treatment; this is assigned to

(36) Liang, A.; Gates, B. C. *J. Phys. Chem. C* **2008**, *112*, 18039.
(37) Fryzuk, M. D.; Johnson, S. A. *Coord. Chem. Rev.* **2000**, *200−202*, 379.
(38) Gambarotta, S.; Scott, J. *Angew. Chem., Int. Ed.* **2004**, *43*, 5298.
(39) Wang, K.; Goldman, A. S.; Li, C.; Nolan, S. P. *Organometallics* **1995**, *14*, 4010.
(40) Geobaldo, F.; Lamberti, C.; Ricchiardi, G.; Bordiga, S.; Zecchina, A.; Turnes Palomino, G.; Otero Areán, C. *J. Phys. Chem.* **1995**, *99*, 11167.
(41) Wang, X. L.; Wovchko, E. A. *J. Phys. Chem. B* **2005**, *109*, 16363.

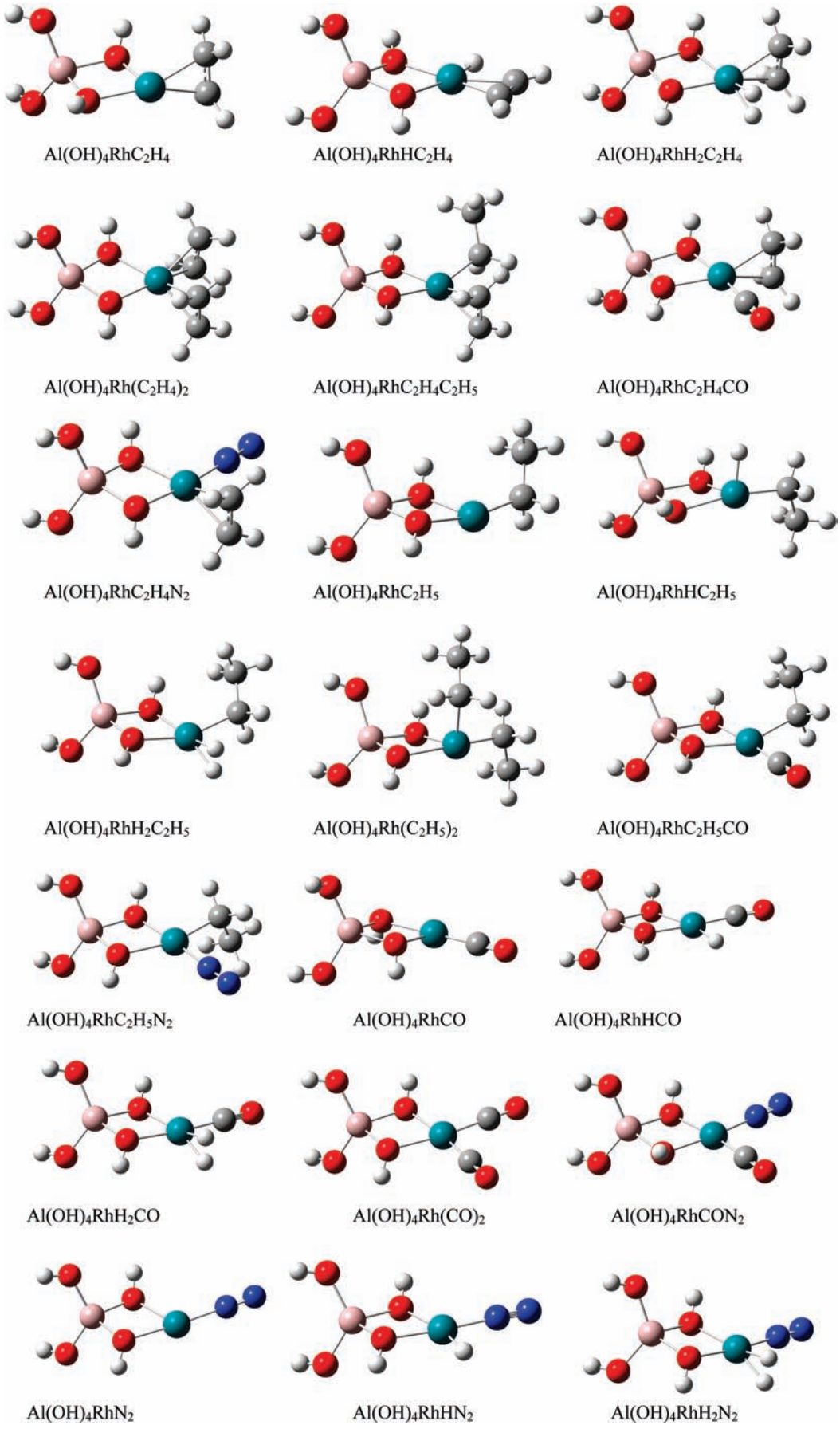

Figure 10. DFT optimized molecular geometries for the model $Al(OH)_4RhL$ and $Al(OH)_4RhLL'$ complexes. Color code: red = O; white = H; pink = Al; blue = Rh; gray = C.

Table 9. Bond Distances (*r*, Å) and the Bond Angle ∠R−Rh−R′ (deg) (R, R′ are Ligands attached to Rh) in Rhodium Complexes

complex	*r*(Rh−H)	*r*(Rh−C)	*r*(Rh−N)	∠R−Rh−R′
$Al(OH)_4RhCO$		1.832		
$Al(OH)_4RhC_2H_4$		2.087(×2), 2.093(×2)		
$Al(OH)_4RhH$	1.517			
$Al(OH)_4RhH_2$	1.537, 1.529			59.9
$Al(OH)_4RhN_2$			1.956	
$Al(OH)_4RhC_2H_5$		1.995		
$Al(OH)_4Rh(CO)_2$		1.851 (×2)		90.0
$Al(OH)_4Rh(C_2H_4)_2$		2.124 (×2), 2.117(×2)		90.1 (×2)
$Al(OH)_4Rh(N_2)_2$			1.915, 1.916	92.4
$Al(OH)_4RhCOH_2$	1.618, 1.622	1.835		89.6, 88.5
$Al(OH)_4RhC_2H_4CO$		2.134 (C_2H_4), 2.141 (C_2H_4), 1.824 (CO)		92.8, 91.8
$Al(OH)_4RhC_2H_4N_2$		2.121, 2.129	1.892	92.5, 91.6
$Al(OH)_4Rh\ N_2H$	1.555		1.926	87.2
$Al(OH)_4RhCOH$	1.558	1.854		83.4
$Al(OH)_4Rh\ C_2H_4H_2$	1.623, 1.621	2.123, 2.127		85.0, 85.3
$Al(OH)_4Rh(C_2H_5)_2$		2.006, 2.018		96.9
$Al(OH)_4RhC_2H_4C_2H_5$		2.135 (C_2H_4), 2.127 (C_2H_4), 2.031 (C_2H_5)		89.2, 92.8
$Al(OH)_4RhCON_2$		1.845	1.924	92.2
$Al(OH)_4RhCOC_2H_5$		1.846 (CO), 2.058 (C_2H_5)		88.1
$Al(OH)_4RhC_2H_5H$	1.518	2.007		85.9
$Al(OH)_4RhC_2H_5N_2$		2.050	1.922	90.2
$Al(OH)_4Rh\ C_2H_4H$	1.548	2.134, 2.147		91.1, 84.8
$Al(OH)_4Rh\ C_2H_5H_2$	1.657, 1.662	2.035		90.4, 83.7
$Al(OH)_4RhN_2H_2$	1.625, 1.620		1.904	89.7, 90.8

the N−N vibration of the $Rh(N_2)$ complex or to the $Rh(N_2)(C_2H_5)$ complex, consistent with the results obtained with $^{15}N_2$. The band at 2214 cm^{-1}, which to the best of our knowledge has not been observed for any supported metal complex, is close to that at 2218 cm^{-1} (which was generally associated with a band at 2244 cm^{-1}), which both Miessner[2] and we observed, as described above. The 2218-cm^{-1} band was assigned by Miessner to the symmetric stretching of N_2 in zeolite-bound $Rh(N_2)_2^+$. According to him, the antisymmetic (A_{as}) and symmetric (A_s) stretching bands of N_2 are evidence of the symmetry in a $Rh(N_2)_2^+$ species (comparable to that of the rhodium *gem*-dicarbonyl). In our experiments, consistent with Miessner's observations and interpretation, a very weak band appeared at 2244 cm^{-1} 30 min after injection of an H_2 pulse into the N_2 stream flowing over the supported rhodium diethylene complex (Figure 7B, spectrum c). The calculated splitting for the asymmetric and symmetric combinations of the N_2 stretches of 36 cm^{-1} is in satisfactory agreement with the experimental splitting of 26 cm^{-1}, being consistent with the differences in the real site and the model cluster used in the calculations.

Because the 2214- and 2244-cm^{-1} bands grew independently of each other and at different rates, they cannot both be assigned to N_2 ligands in $Rh(N_2)_2$; the band at 2214 cm^{-1} grew much faster than the other, and furthermore it disappeared as the other increased in intensity in continuing N_2 flow. Thus, it is clear that these two IR bands arose from separate nitrogen-containing species and that the 2214-cm^{-1} band represents an intermediate in the formation of $Rh(N_2)_2$. Thus, we assign the band at 2214 cm^{-1} to a rhodium complex with only one N_2 ligand, possibly the coordinatively unsaturated $Rh(N_2)$ or the intermediate $Rh(N_2)(C_2H_5)$. This interpretation is consistent with the DFT calculations, which predict a N_2 stretch at 2212 cm^{-1} for the former mono ligand complex and 2214 cm^{-1} for the intermediate complex formed later.

The bands at 2244 and 2218 cm^{-1}, which appeared later when the sample was in flowing N_2 after being exposed to an additional pulse of H_2, are assigned to $Rh(N_2)_2$ because they grew in proportion to each other. Their assignment to a single species is consistent with the observations of Miessner,[2] who reported that the equivalent bands he observed at 2243 and 2217 cm^{-1} should be assigned to $Rh(N_2)_2$ in his rhodium complex supported on DAY zeolite (with a Si/Al atomic ratio of 100) (experiments with $^{15}N_2$ confirmed Miessner's assignments).

The chemistry of the various supported rhodium complexes incorporating nitrogen-containing ligands is summarized in Scheme 1 (these conversions are not stoichiometric).

With the assignment of the 2218- and 2244-cm^{-1} bands to N_2 ligands bonded end-on in $Rh(N_2)_2^+$, the bond angle (α) between the N_2 ligands—calculated on the basis of the relationship $A_{as}/A_{as} = \tan^2(\alpha/2)$—is 92°, smaller than what was observed for the CO ligands in $Rh(CO)_2^+$ (106°). The DFT calculated N_2-Rh-N_2 bond angle is 92.4°.

We concur with Miessner's assignment of a band at 2254 cm^{-1} to the N_2 stretching mode of $Rh(N_2)(CO)$.[2] This assignment was confirmed by exchange experiments carried out with $^{15}N_2$ and $C^{18}O$, as well as a multivariate correlation analysis.[2] A similar conclusion was drawn by Wang et al.[41] for a sample formed from $Rh(CO)_2$ bonded to zeolite Y, which was characterized by IR spectroscopy during photolysis with ultraviolet light. Wang et al. showed that the zeolite-supported rhodium carbonyl species prepared by Miessner's method, after photolysis, was reactive in N_2. The assignment of bands at 2252 and 2062 cm^{-1}, observed when the sample was in contact with N_2 during photolysis to give $Rh(N_2)(CO)$ species, was confirmed in experiments with ^{13}CO. The DFT-calculated frequencies for the various species shown in Scheme 1 are completely consistent with these assignments.

Stability of Supported Rhodium Complexes with Nitrogen Ligands. As shown in Figure 7, the formation of rhodium−N_2 species was rapid, occurring within seconds after exposure of the supported sample to N_2 at 298 K, as shown by the band at 2214 cm^{-1}. The narrowness of this band indicates the formation of nearly uniform species. However, the intensity of the band decreased rapidly with continuing flow of N_2, indicating that the initially formed species were not stable at 298 K and reacted to form other surface species. In contrast, the rhodium complexes with two N_2 ligands are stable at 298 K, as evidenced by their

intensities, which increased when the sample was in flowing N_2. The stability of the rhodium dinitrogen complexes was also demonstrated by Miessner; his $Rh(N_2)_2$ structure was stable at temperatures up to 473 K in N_2.[2]

Conclusions

Well-defined rhodium complexes with ethylene ligands were formed from $Rh(C_2H_4)_2(acac)$ on dealuminated zeolite Y and found to be highly reactive in various gas atmospheres in a flow reactor. IR spectroscopy and mass spectrometry with isotopically labeled compounds were used to monitor the reactions, and the assignments of the vibrational spectra were validated with DFT calculations, and some of the structures required theory for their determination. The ethylene ligands bonded to the rhodium were readily exchanged with deuterated ethylene at 298 K. The ethylene complexes reacted with CO to form site-isolated rhodium *gem*-dicarbonyls, consistent with the DFT bond energy calculations. Supported rhodium dinitrogen species formed when the rhodium diethylene complex was in contact with N_2 in the presence of H_2 at 298 K, and the N_2 ligands were bonded end-on to the rhodium. H_2 reacts with the activated ethylene ligands on Rh to produce C_2H_5 ligands bonded to the Rh, leading to the catalytic production of ethane. The vibrational spectra indicate the formation of a rhodium hydride species in our experiments.

Experimental and Calculational Section

Materials and Sample Preparation. Details of the sample preparation have been reported.[5] Sample syntheses and handling were performed with the exclusion of moisture and air by use of standard Schlenk line techniques and inert-atmosphere gloveboxes. The supported rhodium complex was prepared by bringing the precursor $Rh(C_2H_4)_2(C_5H_7O_2)$ [acetylacetonatobis(ethylene)rhodium(I)] (Strem, 99%) in contact with highly dealuminated HY zeolite (DAY zeolite) (Zeolyst International) in dried and deoxygenated *n*-pentane (Fisher, 99%). The zeolite, with a Si/Al atomic ratio of approximately 30, was calcined in flowing O_2 at 773 K for 4 h and then evacuated for 16 h at 773 K prior to being brought in contact with the precursor in *n*-pentane solvent. H_2 was supplied by Airgas (99.995%) or generated by electrolysis of water in a Balston generator (99.99%) and purified by passage through traps containing reduced Cu/Al_2O_3 and activated zeolite 4A to remove traces of O_2 and moisture, respectively. He (Airgas, 99.997%) and C_2H_4 (Airgas, 99.99%) were purified by passage through similar traps. The following gases were all supplied by Cambridge Isotope Laboratories: D_2 (99.8%), C_2D_4 (98%), ^{13}CO (99.9%), $H_2{}^{18}O$ (98.1%), and $^{15}N_2$ (99.8%); these were used as received.

IR Spectroscopy. A Bruker IFS 66v/S spectrometer with a spectral resolution of 2 cm^{-1} was used to collect transmission IR spectra of zeolite-supported rhodium samples. In an N_2- or argon-filled glovebox, each sample (typically, 20 mg), handled with exclusion of moisture and air, was pressed into a thin wafer and loaded into the cell (In-situ Research Institute, South Bend, IN) through which reactive gases flowed. The cell was connected to a vacuum system with a base pressure of 10^{-4} bar, which allowed recording of spectra while the reactant gases (He, H_2, D_2, C_2H_4, C_2D_4, N_2, $^{15}N_2$, CO, or He mixed with ^{13}CO) flowed through the cell at 298 K and atmospheric pressure. Each spectrum is the average of a number of scans, ranging from 8 to 128.

Mass Spectrometry. Mass spectra of the gases introduced into the flow system and the effluents produced by reaction with the sample were measured with an online Balzers OmniStar mass spectrometer running in multi-ion monitoring mode; these data were recorded simultaneously with the IR spectra. Specifically, changes in the signal intensities of the major fragments of C_2H_4 (m/e = 26, 27, and 28), C_2H_6 (m/e = 26, 27, 28, and 30), and N_2 (m/e = 14 and 28) were recorded.

X-ray Absorption Spectroscopy. The X-ray absorption spectra were recorded at X-ray beamline MR-CAT at the Advanced Photon Source (APS) at the Argonne National Laboratory. The storage ring electron energy and ring currents were 7.0 GeV and 105 mA, respectively. The cryogenic double-crystal Si(111) monochromator was detuned by 15−20% at the Rh K edge to minimize the effects of higher harmonics in the X-ray beam.

In an argon-filled glovebox at the APS, the zeolite-supported rhodium samples were pressed into self-supporting wafers. Each wafer was loaded into a flow-through cell,[42] and the cell was sealed in the inert atmosphere. The mass of each wafer (approximately 0.5 g) was chosen to yield optimal absorption measurements at the Rh K edge (23 220 eV) (giving an X-ray absorbance of approximately 2.0 calculated at an energy 20 eV greater than the absorption edge).

X-ray absorption spectra were recorded with a rhodium foil and each sample at 298 K and atmospheric pressure in the presence of ethylene for 1 h. The partial pressure of C_2H_4 in the gas stream was 55 mbar (with the balance being He), with a total gas flow rate of 35 mL/min. All spectra were collected in transmission mode during the treatments, and a spectrum was recorded every 3 min.

EXAFS Data Analysis. The X-ray absorption edge energy was calibrated with the measured signal of a rhodium foil (scanned simultaneously with the sample) at the Rh K edge, which was taken to be the inflection point at 23 220 eV. The data were normalized by dividing the absorption intensity by the height of the absorption edge.

Analysis of the EXAFS data was carried out with the software ATHENA of the IFEFFITP[43,44] package and the software XDAP. ATHENA was used for edge calibration, deglitching, data normalization, and conversion of the data into an EXAFS (χ) file. A background function was subtracted from the normalized data by using spline points between the values of the wave vector (k) of 1.2 and 15.9 $Å^{-1}$, with a strong spline clamp made to the end point. An R_{bkg} value (the value at which ATHENA removes the low-frequency Fourier components) in the range of 1.0 to 1.1 (typical for removal of background noise) was used for all spectra. XDAP allowed the efficient application of a difference-file technique[45,46] for determination of optimized fit parameters.

Structural models postulated for the supported rhodium species were compared with the EXAFS data; the models included the plausible contributions Rh−Rh, Rh−Al, Rh−O, and Rh−C. Reference files, with backscattering amplitudes and phase shifts for Rh−Rh, Rh−Al, Rh−O, and Rh−C contributions, were calculated with the software FEFF7.0[47] from crystallographic coordinates of the unit cells of the reference compounds rhodium metal[48] (for the Rh−Rh contribution), Rh−Al alloy[49] (for the Rh−Al contribution), and $Rh(C_2H_4)_2(acac)$[50] (for the Rh−O and Rh−C contributions).

Analysis was carried out with unfiltered data; iterative fitting was performed until optimum agreement was attained between the calculated k^0-, k^1-, k^2-, and k^3-weighted EXAFS data and each postulated model. The data were fitted in r space with the Fourier-transformed χ data (r is the distance from the absorbing Rh atom; χ is the EXAFS function). The EXAFS data were analyzed with 12 free parameters over the ranges $3.60 < k < 12.05$ $Å^{-1}$ and $1.2 < r < 4.0$ Å. The number of parameters used in the fitting was always less than the statistically justified number, computed with the

(42) Odzak, J. F.; Argo, A. M.; Lai, F. S.; Gates, B. C.; Pandya, K.; Feraria, L. *Rev. Sci. Instrum.* **2001**, *72*, 3943.
(43) Newville, M.; Ravel, B.; Haskel, D.; Rehr, J. J.; Stern, E. A.; Yacoby, Y. *Physica B* **1995**, *208/209*, 154.
(44) Newville, M. *J. Synchrotron Rad.* **2001**, *8*, 96.
(45) Kirlin, P. S.; van Zon, F. B. M.; Koningsberger, D. C.; Gates, B. C. *J. Phys. Chem.* **1990**, *94*, 8439.
(46) van Zon, J.; B, A. D.; Koningsberger, D. C.; van't Blik, H. F. J.; Sayers, D. E. *J. Chem. Phys.* **1985**, *82*, 5742.
(47) Zabinsky, S. I.; Rehr, J. J.; Ankudinov, A.; Albers, R. C.; Eller, M. J. *Phys. Rev. B* **1995**, *52*, 2995.
(48) Singh, H. P. *Acta Crystallogr., Sect. A* **1968**, *A 24*, 469.

Nyquist theorem: $n = (2\Delta k \Delta r/\pi) + 1$, where Δk and Δr, respectively, are the k and r ranges used in the fitting.[51]

The initial fitting was carried out with the plausible absorber-backscatterer contributions: Rh−Rh, Rh−O, Rh−C, and Rh−Al. No Rh−Rh contribution was detected in the fitting, and no fit with only two contributions was adequate. The final fit includes the following contributions: Rh−O, Rh−C, and Rh−Al. It is not surprising that the Rh−Al contribution is indicated for the supported mononuclear species, as the charge-compensating cationic rhodium is expected to be associated with the aluminum sites, as discussed elsewhere.[4]

Calculations. . Density functional theory calculations with the B3LYP exchange correlation functional[52,53] and the aug-cc-pVDZ and aug-cc-pVDZ-PP basis sets[54,55] were used to optimize the geometries and to predict the vibrational frequencies for various isotopic substitution patterns for a model of Rh^+ binding to the acidic site in the zeolite. The simple model is $Al(OH)_4RhL_1L_2$, where L_1 and L_2 are the different ligands C_2H_4, H_2, N_2, CO, H, and C_2H_5. Such a simplified representation of rhodium complexes in the zeolite has been shown be provide a good representation of the geometry and ^{13}C NMR chemical shifts characteristic of similar complexes.[9] We chose this simple model for efficiency, because our goal was to explore a wide range of ligand combinations.

For L_1, L_2 = any combination of C_2H_4, H_2, N_2, CO, and N_2, the lowest-lying electronic state is a singlet state. For L_1 a combination of any of the just-stated ligands and L_2 = H or C_2H_5, the electronic state is a doublet. If L_1 and L_2 are H and/or C_2H_5, the electronic state is a singlet. For a single ligand, the ground state is singlet for C_2H_4, H_2, N_2, and CO and a triplet for L = N_2. The ground state is a doublet for a single H or C_2H_5 ligand (see Supporting Information).

The calculated harmonic frequencies of the diatomics were scaled to experimental values[56] for H_2, N_2, and CO and the C−H/C−D and C=C stretching frequencies were scaled to the appropriate experimental values[57] for C_2H_4, C_2D_4, C_2H_6, and C_2D_6. The resulting scale factors were used to scale the appropriate frequencies in the supported rhodium complexes. The calculated and experimental frequencies as well as the scaling factors are given in Supporting Information, as are the molecular coordinates. The molecular structures of the ligands bonded to the rhodium complexes are shown in Figure 10, and the critical geometry parameters characterizing the ligand bonding to the metal are shown in Table 9.

Acknowledgment. The research was supported by the U.S. Department of Energy, Office of Science, Basic Energy Sciences, Grants DE-FG02-04ER15600 at the University of California, DE-FG02-03ER15481 at the University of Alabama, and DE-FG02-04ER15598 at the University of Southern California. A.L. thanks Chevron for a fellowship, and D.A.D. thanks the Robert Ramsay Fund at the University of Alabama for partial support. We acknowledge beam time and the support of the DOE Division of Materials Sciences for its role in the operation and development of beamline MR-CAT at the Advanced Photon Source at the Argonne National Laboratory.

Supporting Information Available: Tables for generating the vibrational frequency scale factors. Tables of calculated vibrational frequencies for C−H, C=C, Rh−H, and Rh−N_2, frequencies for σ and π bonding motifs for $Al(OH)_4Rh(N_2)_2$ complexes. Molecular coordinates and total energies including singlet−triplet and doublet−quartet splittings. Single ligand dissociation energies for the ^4Rh, $^3Rh^+$, and $^3Al(OH)_4Rh$ complexes. This material is available free of charge via the Internet at http://pubs.acs.org.

JA900041N

(49) Donney, J. D. H.; Ondik, H. M. *Crystal Data Determinative Tables*, 3rd ed.; U.S. Department of Commerce, National Bureau of Standards and the Joint Committee on Powder Diffraction Standards: Washington, DC, 1973; Vol. II, pC−4.
(50) Bühl, M.; Håkansson, M.; Mahmoudkhani, A. H.; Öhrström, L. *Organometallics* **2000**, *19*, 5589.
(51) Lytle, F. W.; Sayers, D. E.; Stern, E. A. *Physica B* **1989**, *158*, 701.
(52) Becke, A. D. *J. Chem. Phys.* **1993**, *98*, 5648.
(53) Lee, C.; Yang, W.; Parr, R. G. *Phys. Rev. B* **1988**, *37*, 785.
(54) (a) Dunning, T. H., Jr. *J. Chem. Phys.* **1989**, *90*, 1007. (b) Kendall, R. A.; Dunning, T. H., Jr.; Harrison, R. J. *J. Chem. Phys.* **1992**, *96*, 6796. (c) Woon, D. E.; Dunning, T. H., Jr. *J. Chem. Phys.* **1993**, *98*, 1358. (d) Dunning, T. H., Jr. *J. Phys. Chem. A* **2000**, *104*, 9062.
(55) (a) Peterson, K. A. *J. Chem. Phys.* **2003**, *119*, 11099. (b) Peterson, K. A.; Figgen, D.; Goll, E.; Stoll, H.; Dolg, M. *J. Chem. Phys.* **2003**, *119*, 11113. (c) Peterson, K. A.; Puzzarini, C. *Theor. Chem. Acc.* **2005**, *114*, 283. (d) Peterson, K. A.; Figgen, D.; Dolg, M.; Stoll, H. *J. Chem. Phys.* **2007**, *126*, 124101. unpublished basis sets for the first and third row transition elements. (e) Peterson, K. A. In *Annual Reports in Computational Chemistry*, Vol. 3. Spellmeyer, D. C.; Wheeler, R. A. Eds. Elsevier, B. V. Amsterdam, The Netherlands, 2007.
(56) Huber, K. P.; Herzberg, G. *Constants of Diatomic Molecules. Molecular Spectra and Molecular Structure, Vol. IV*, Van Nostrand, Princeton, 1979.
(57) Shimanouchi, T. *Tables of Molecular Vibrational Frequencies Consolidated Volume I*, NSRDS-NBS 39, National Bureau of Standards, Washington, D.C., 1972.